Islamic Azad University

Journal of

Optoelectronical Nanostructures

Volume 10, Issue 2, Summer 2025, Page 71-83

Research Paper

Sensitivity enhancement of a bimetallic surface plasmon resonance biosensor

Hassan Zahmatkeshan[1], Mohammad Javad Karimi *[2], Mojtaba Sadeghi[1], Zahra Adelpour[1]

[1] Department of Electrical Engineering, Shi.C., Islamic Azad University, Shiraz, Iran

[2] Department of Physics, Shiraz University of Technology, Shiraz, Iran

Received: 2025.04.14
Revised: 2025.08.11
Accepted: 2025.08.14
Published: 2025.08.25

Use your device to scan and read the article online

Keywords:
Biosensor,
Sensitivity,
Surface plasmon resonance

Abstract:

In this study, a plasmonic biosensor with a kreschmann configuration is evaluated by changing the sensing medium's refractive index from 1.330 to 1.335, which includes BK7, gold/silver, silicon, nickel, hexagonal boron nitride, black phosphorus/transition-metal dichalcogenides and sensing medium layers. The sensitivity, figure of merit, quality factor and detection accuracy are the biosensor performance characteristics and are checked at the 633 nm wavelength. The effects of gold and silver layers on the transition-metal dichalcogenides and black phosphorus layers are investigated separately and their performance parameters have been calculated numerically. Since the highest sensitivity is related to the Ag metal with the BP layer, the minimum reflectance and sensitivity as a function of the thickness and number of layers for this structure are examined. The sensitivity of the proposed biosensor (504 deg.RIU^{-1}) is approximately 1.5 times higher than the highest sensitivity reported in comparable studies.

Citation: H. Zahmatkeshan, M. J. Karimi, M. Sadeghi, Z. Adelpour. Sensitivity enhancement of a bimetallic surface plasmon resonance biosensor. **Journal of Optoelectronical Nanostructures.** 2025; 10(2): 71-83.

***Corresponding author:** Mohammad Javad Karimi
Address: Department of Physics, Shiraz University of Technology, Shiraz, Iran
Email: karimi@sutech.ac.ir
DOI: https://doi.org/10.71577/jopn.2025.1203950

1. INTRODUCTION

Plasmonics plays a significant role in the design of biosensors [1] and photovoltaic cells [2]. Surface plasmon resonance (SPR) biosensors can detect biomaterials, making them valuable for medical diagnostics [3] and food safety [4] applications. These biosensors can identify analytes with minimal changes in their refractive index (RI) [5], achieving high accuracy [6] and sensitivity [7] in real-time [8]. Additionally, they are cost-effective [9] and do not require professional personnel for operation [10].

The sensing medium's (SM) RI changes leads to the resonance angle shifts [11]. In SPR sensors that utilize multilayer structures, the Kretschmann [12] and Otto [13] configurations are commonly employed. A thin air gap separates the metal layer from the prism in the Otto configuration, while in the Kretschmann geometry, the prism and the metal layer are in direct contact. Due to the coupling of transverse magnetic (TM) waves or p-polarized incident light with the free electrons on the metal surface, surface plasmons are excited at the metal-dielectric interface [13,14]. Silver (Ag) [15], gold (Au) [16], copper (Cu) [17], aluminum (Al) [18], and nickel (Ni) [19] are recognized as materials with plasmonic properties that can enhance surface plasmon signals in sensors [20].

Conventional sensors sensitivity, comprising a prism, metal layer, and SM [21], achieve a peak reported value of 116 deg RIU^{-1} [22], which is due to the weak adhesion of the metal layer to the SM [23] resulting in very low sensitivity [24]. Recently, to enhance the sensitivity of these sensors, two-dimensional (2D) nanomaterials such as black phosphorus (BP) [25], graphen (Gr) [5], Mxene [22], transition-metal dichalcogenides (TMDCs) [26], and hexagonal boron nitride (h-BN) [27] are used between the metal layer and the SM. Also, using an antireflection layer like MgF_2 enhances light absorption in the biosensor, increasing sensitivity [28]. The general form of TMDCs is MX_2 where M represents a metal of transition such as Tungsten (W) and Molybdenum (Mo), and X shows materials of chalcogen like Sulphur (S) and Selenium (Se) [29]. These materials are molybdenum disulfide (MoS_2), tungsten disulfide (WS_2) molybdenum diselenide ($MoSe_2$) and tungsten diselenide (WSe_2).

The use of 2D nanomaterials in SPR sensors, biosensors, and solar cells has grown recently. For instance, Panda et al. designed a plasmonic biosensor for malaria pathogen detection, utilizing a CaF2 prism, titanium oxide, Ag, platinum diselenide, WS2, and SM layers, achieving a maximum sensitivity of 240.10 deg. RIU^{-1} [30]. Similarly, Kumar et al. analyzed a biosensor for carcinoembryonic antigen (CEA) detection, composed of a prism of BK7, titanium, Ag, MoS2, Gr, and SM layers, reporting a peak sensitivity of 144.72 deg. RIU^{-1} [31]. Daher et al. investigated a BAK1 prism-based structure with Ag, bismuth ferrite, BP, and SM

layers, yielding a 358 deg. RIU^{-1} sensitivity [32]. Furthermore, Kalpana et al. presented an SPR sensor for colorectal detection, incorporating a CaF2 prism, Ag, MXene, h-BN, BP, and SM layers, and achieving a 315 deg. RIU^{-1} sensitivity [27].

This study investigates a biosensor of SPR with a prism of BK7 and layers of Ag, Si, Ni, h-BN, BP, and SM. We also explore substituting Au for Ag and TMDCs for BP. Ag offers a cost-effective alternative to Au with comparable accuracy [33]. A narrower full width at half maximum (FWHM) in the reflectance curve shows superior sensor performance. Incorporating a high refractive index Si layer (BK7/Ag/Si/SM) enhances sensitivity compared to the conventional BK7/Ag/SM sensor [11]. The h-BN layer's high-temperature stability and chemical resistance make it suitable for SPR sensors. BP, with its 0.53 nm thickness and desirable bio-recognition element (BRE) properties [27], effectively captures biomolecules [34] due to its high surface-to-volume ratio [35], bandgap of tunable [24], and low thermal conductivity [36], which further increases sensitivity.

The biosensor's performance, comprising sensitivity (S), detection accuracy (DA), quality factor (QF), and figure of merit (FOM), was evaluated using attenuated total reflection (ATR) at the visible 633 nm wavelength (TM-polarized Helium-Neon laser).

2. DESIGN AND MODELING

Figure 1 depicts a biosensor of SPR with seven layers designed in a Kretschmann geometry.

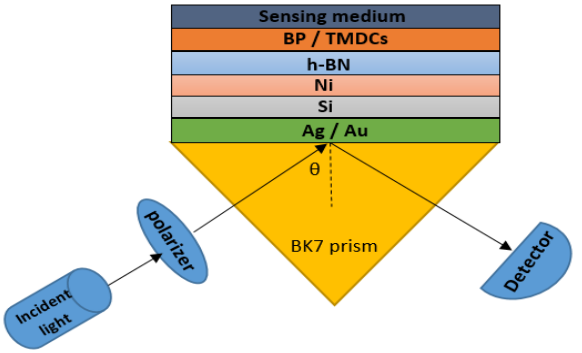

Fig. 1. The proposed SPR biosensor

The coupling of light to the surface plasmon polaritons (SPPs) occurs through the BK7 prism, and its RI is given by [37,38].

$$n_{BK7} = \left(\frac{\alpha_1 \lambda^2}{\lambda^2 - \beta_1} + \frac{\alpha_2 \lambda^2}{\lambda^2 - \beta_2} + \frac{\alpha_3 \lambda^2}{\lambda^2 - \beta_3} + 1\right)^{\frac{1}{2}} \quad (1)$$

where λ is the incident light wavelength, and α_1 = 1.03961212, α_2 = 0.231792344, α_3 = 1.0104694, β_1 = 0.00600069867, β_2 = 0.0200179144, and β_3 = 103.560653.

The RI of the metal layers is presented by the Drude–Lorentz model as follows [39]:

$$n_{metal} = \left(1 - \frac{\lambda^2 * \lambda_c}{\lambda_p^2 (\lambda_c + \lambda * i)}\right)^{\frac{1}{2}} \quad (2)$$

The parameters of wavelength of plasma (λ_p) and wavelength of collision (λ_c) for Ag, Au and Ni are listed in Table 1.

Table1. λ_p and λ_c for Ag, Au and Ni at the wavelength of 633 nm

Metal	$\lambda_p(m)$	$\lambda_c(m)$
Ag	1.4541×10^{-7}	1.7614×10^{-5}
Au	1.6826×10^{-7}	8.9342×10^{-6}
Ni	2.5381×10^{-7}	2.8409×10^{-5}

The RI of the Si and SM are 3.9160 and $n = 1.33$, respectively. Table 2 lists the RI and monolayer thickness of the 2D materials used in the biosensor.

Table2. RI and monolayer thickness of the 2D nanomaterials

2D nanomaterials	RI (λ=633 nm)	Monolayer thickness (nm)
h-BN	1.65	1
BP	3.5+0.01i	0.53
MoS_2	5.0805+1.1723i	0.65
$MoSe_2$	4.6226+1.0063i	0.70
WS_2	4.8937+0.3124i	0.80
WSe_2	4.5501+0.4332i	0.70

The intensity of reflected light is calculated using the transfer matrix method (TMM), as given by [37],

$$M_{ij} = \left(\prod_{k=2}^{N-1} M_k\right)_{ij} = \begin{pmatrix} M_{11} & M_{12} \\ M_{21} & M_{22} \end{pmatrix} \quad (3)$$

$$M_k = \begin{bmatrix} \cos\beta_k & -(i \sin\beta_k)/q_k \\ -iq_k \sin\beta_k & \cos\beta_k \end{bmatrix} \quad (4)$$

$$q_k = \frac{(\varepsilon_k - n_1^2 sin^2\theta_1)^{1/2}}{\varepsilon_k} \quad (5)$$

$$\beta_k = \frac{2\pi d_k}{\lambda}(\varepsilon_k - n_1^2 sin^2\theta_1)^{1/2} \quad (6)$$

In the above equations, θ_1, n_1, ε_k, and d_k are the incident angle, RI of the prism, permittivity and thickness of the k-th layer, respectively.

The amplitude reflection coefficient is r_p:

$$r_p = \frac{(M_{11} + M_{12}q_N)q_1 - (M_{21} + M_{22}q_N)}{(M_{11} + M_{12}q_N)q_1 + (M_{21} + M_{22}q_N)} \quad (7)$$

And the reflectance coefficient:

$$R_p = |r_p^2| \quad (8)$$

Biosensor performance characteristics are S, R_{min}, DA, QF, and the FOM. The sensitivity (S) is given by,

$$S = \frac{\Delta\theta_{SPR}}{\Delta n} \quad (deg.RIU^{-1}) \quad (9)$$

where $\Delta\theta_{SPR}$ is the shift in the resonance angle, and $\Delta n = 0.005$ is the RI change of the SM, respectively. The resonance angle (θ_{SPR}) is the angle at which the dip appears in the reflectance spectrum. Additionally, the reflectance at the bottom of the dip, denoted as R_{min}, represents the minimum value of the reflectance. DA, QF, and the FOM are defined as follows:

$$DA = \frac{1}{FWHM} \quad (deg^{-1}) \quad (10)$$

$$QF = \frac{S}{FWHM} \quad (RIU^{-1}) \quad (11)$$

$$FOM = S \times \frac{1 - R_{min}}{FWHM} \quad (RIU^{-1}) \quad (12)$$

3. RESULTS AND DISCUSSION

We studied an SPR biosensor comprising a prism of BK7, Ag/Au, Si, Ni, h-BN, BP/TMDCs, and SM layers. For these ten structures (two metals (Ag and Au) and five 2D material (BP, MoS2, MoSe2, Ws2, WSe2)), the effects of layer thickness (d_{layer}) and the number of layers (L) on the performance characteristics of the biosensor are analyzed. The three-layer structure consisting of Si, Ni, and h-BN is present in all ten examined configurations.

Table 3 lists the optimal layer thicknesses for maximum biosensor sensitivity. For example, row one of the Table denotes that the optimal thicknesses and the number of layer for the Au/ Si/Ni/ h-BN/ BP structure are 16 nm/ 5 nm/ 39 nm/ 1

L/ 2L, respectively. The comparison of the rows in the table indicates that structures containing silver exhibit greater sensitivity than those that include gold. Additionally, structures incorporating BP show higher sensitivity compared to TMDC structures. Among the TMDCs, the structures made of Tungsten provides greater sensitivity for the sensor.

Table 3: The performance parameters (S, FOM, QF, DA & R_{min}) of the designed structures with Ag/Au (column 1) and 2D nanomaterials of BP/TMDCs (column 3).

Type and thickness (nm)	Si(nm) /Ni(nm)/ h-BN(L)	Type and number of layers	S (deg.RIU^{-1})	FOM (RIU^{-1})	QF (RIU^{-1})	DA (deg.$^{-1}$)	R_{min}
Au: 16	5/39/1	BP: 2	492	80.40	81.44	0.1655	0.0127
Au: 10	5/38/1	MoS_2: 1	288	28.95	29.38	0.1020	0.0149
Au: 10	5/39/1	$MoSe_2$: 1	300	31.82	32.11	0.1071	0.0092
Au: 7	5/39/1	WS_2: 1	368	41.78	43.60	0.1185	0.0418
Au: 8	5/39/3	WSe_2: 1	382	47.31	47.31	0.1239	0.0002
Ag: 16	**5/36/2**	**BP: 2**	**504**	**84.06**	**84.24**	**0.1672**	**0.0021**
Ag: 10	5/39/1	MoS_2: 1	290	29.26	30.18	0.1041	0.0305
Ag: 10	5/39/1	$MoSe_2$: 1	300	32.16	32.46	0.1082	0.0091
Ag: 10	5/39/1	WS_2: 1	396	50.62	50.64	0.1279	0.0003
Ag: 8	5/39/3	WSe_2: 1	384	47.46	47.49	0.1237	0.0005

Overall, Table 3 indicates that the optimized biosensor is the BK7/Ag/Si/Ni/ h-BN/ BP structure with performance parameters; S (504 deg. RIU^{-1}), FOM (84.06 RIU^{-1}), QF (84.24 RIU^{-1}) and DA (0.1672 deg.$^{-1}$). The corresponding optimal thicknesses and number of layers are Ag (16 nm), Si (5 nm), Ni (36 nm), h-BN (2 layers), and BP (2 layers). Therefore, we focused on the BK7/Ag/Si/Ni/h-BN/BP/SM structure and examined four layout scenarios; i) Ag/Si, ii) Ag/Si/Ni, iii) Ag/Si/Ni/h-BN and iv) Ag/Si/Ni/h-BN/BP. Figure 2 illustrates the SPR reflectance curve for these configurations. This figure shows that adding layers increases both the depth and angular shift of the reflectance dip, enhancing the sensor's operational parameters. Additionally, Table 4 presents the thickness and number of layers and performance parameters for these configurations. The table demonstrates that adding a Ni layer to the first structure, h-BN to the second, and BP to the third enhances sensitivity. The fourth structure's sensitivity (504 deg RIU^{-1}) is 100% higher than the second structure's (250 deg RIU^{-1}).

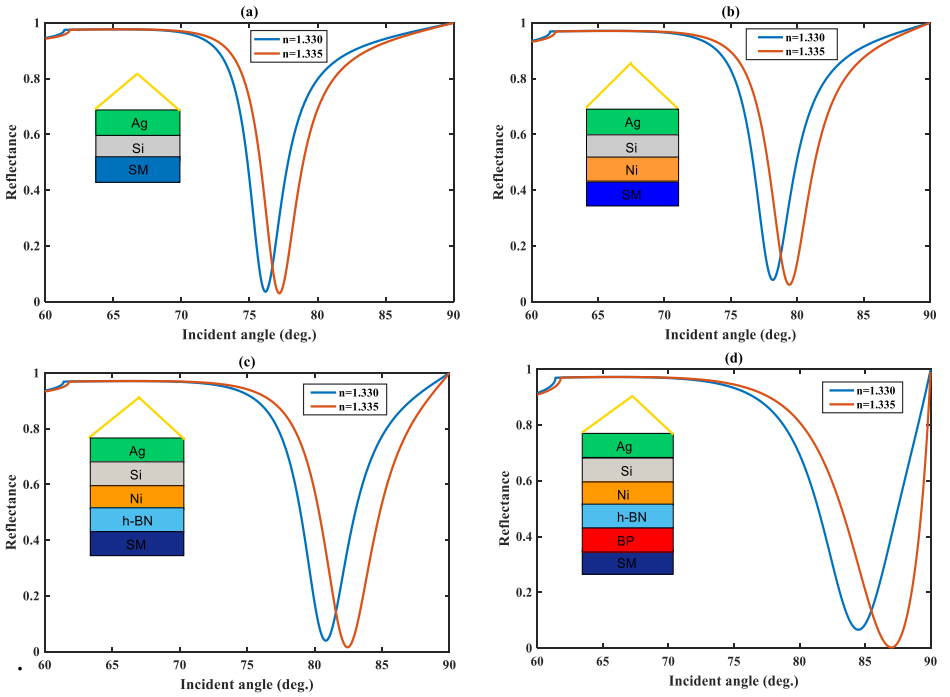

Fig. 2. The reflectance curve for (a) Ag/Si, (b) Ag/Si/Ni, (c) Ag/Si/Ni/h-BN, (d) Ag/Si/Ni/h-BN/BP structures

Table 4. The thickness, number of layers, and performance parameters for (i) Ag/Si, (ii) Ag/Si/Ni, (iii) Ag/Si/Ni/h-BN, (iv) Ag/Si/Ni/h-BN/BP structures

Structure	**Ag**d_{Ag} (nm)	**Si**d_{Si} (nm)	**Ni**d_{Ni} (nm)	**h-BN**	**BP**	**S** deg. RIU^{-1}	**FOM** RIU^{-1}	**QF** RIU^{-1}	**DA** deg.$^{-1}$	R_{min}
i	50	5	-	-	-	204	62.11	64.06	0.3140	0.0304
ii	20	5	39	-	-	250	64.14	68.31	0.2733	0.0610
iii	20	5	39	3 L	-	328	71.88	72.84	0.2221	0.0133
iv	16	5	36	2 L	2 L	504	84.06	84.24	0.1672	0.0021

Figure 3 presents the minimum reflectance (R_{min}) and sensitivity (S) of the fourth structure (Ag/Si/Ni/h-BN/BP) as a function of layer thickness and the number of layers. In Figures 3(a)-(e), one parameter varies while the others remain constant, as taken from row 4 of Table 4.

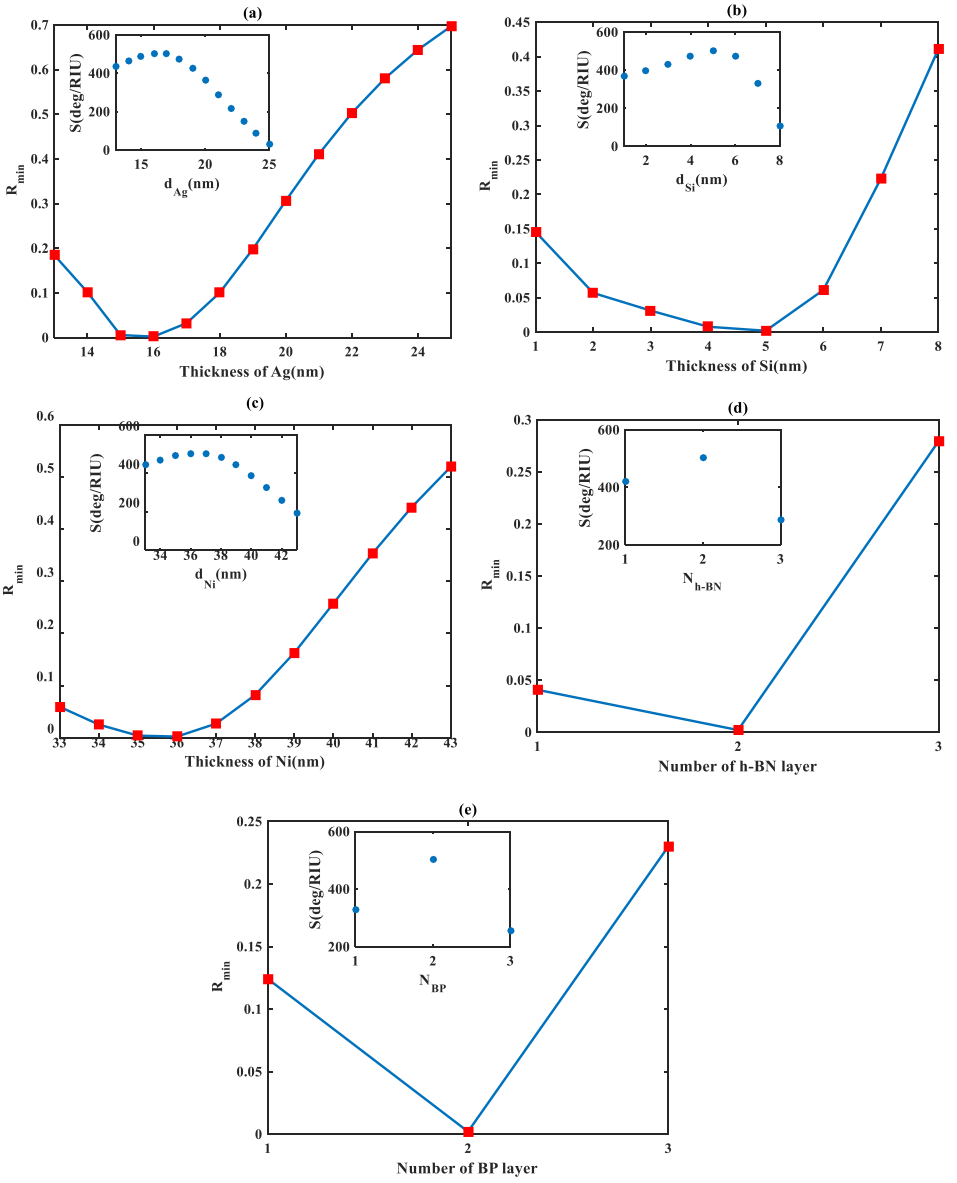

Fig. 3: R_{min} versus (a) the thickness of Ag layer, (b) the thickness of Si layer, (c) the thickness of Ni layer, (d) the number of h-BN layer, (e) the number of BP layer. The inset figures show the sensitivity

Figure 3 shows that the optimal performance, characterized by the highest sensitivity and lowest R_{min}, occurs with a 16 nm Ag layer (see Fig. 3(a)), a 5 nm Si layer (see Fig. 3(b)), and a 36 nm Ni layer (see Fig. 3(c)). As shown in Figures 3(d) and 3(e), a structure with 2 h-BN layers and 2 BP layers yields the highest sensitivity.

For the Ag/Si/Ni/h-BN/BP structure, we generalized the RI of the SM from 1.330 to 1.345 and obtained the S, R_{min}, QF and DA, as illustrated in Figs. 4(a) and 4(b). This figure shows that these parameters exhibit nonmonotonic behaviors with the RI. As RI increases, S, QF, and DA initially increase, reach a maximum, and then decrease, while R_{min} exhibits the opposite trend.

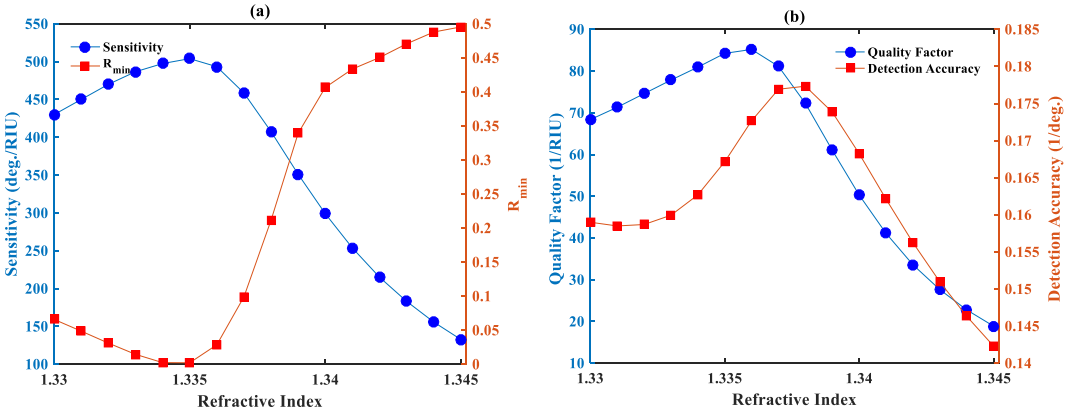

Fig. 4. (a) Sensitivity and R_{min}, (b) QF and DA versus the sensing RI

In Table 5, we compared the performance characteristics of our designed structures with previously reported studies. Our proposed SPR biosensors, incorporating gold (Au) and silver (Ag) layers along with black BP, exhibited sensitivities of 492 and 504 deg. RIU^{-1}, respectively. These values are significantly higher than those reported in Refs. [11], [27], [32] and [40].

Table 5: performance characteristics comparison of our designed structures with previously published devices

SPR sensor configuration	S deg.RIU^{-1}	QF RIU^{-1}	DA deg.$^{-1}$	R_{min}	Ref.
BK7/Ag/Si/Franckeite	305	52	0.1700	-	[11]
CaF2/Ag/MXene/h-BN/BP	315	52.34	0.1660	-	[27]
BAK1/Ag/$BiFeO_3$/BP	358	-	-	-	[32]
CaF2/Ag/$BaTiO_3$/Ni/MXene	316	97.07	0.3072	0.480	[40]
BK7/Au/Si/Ni/h-BN/BP	**492**	**81.44**	**0.1655**	**0.012**	**This work**
BK7/Ag/Si/Ni/h-BN/BP	**504**	**84.24**	**0.1672**	**0.002**	**This work**

4. CONCLUSION

Our proposed biosensors included BK7, Ag/Au, Si, Ni, h-BN, BP/TMDCs (MoS_2, $MoSe_2$, WS_2 and WSe_2) and SM layers. The Si, Ni and h-BN are common in all structures. We investigated the effects of Au and Ag layers on the BP and TMDCs layers, separately. The highest sensitivities are 492 and 504 deg. RIU^{-1} respectively, related to Au and Ag layers along with 2 BP layers. Since the best performance (S=504 deg. RIU^{-1}, FOM=84.06 RIU^{-1}, QF=84.24 RIU^{-1} and DA=0.1672 $deg.^{-1}$) of the biosensor corresponds to the Ag layer with the BP layer, the thickness and number of layers in this structure were examined. The optimal thicknesses and layers are: Ag (16 nm), Si (5 nm), Ni (36 nm), h-BN (2 layers), and BP (2 layers). All proposed biosensors can be used in biomedical applications.

REFERENCES

[1] Nasrolahi M, Farmani A, Horri A, Hatami H (2024) FDTD Analysis of a High-sensitivity refractive index sensing based on Fano resonances in a plasmonic planar split-ring resonators. Journal of Optoelectronical Nanostructures. 9(3). https://doi.org/10.30495/JOPN.2024.33499.1321

[2] Abdolahzadeh Ziabari A, Royanian S, Yousefi R, Ghoreishi S (2020) Performance improvement of ultrathin CIGS solar cells using Al plasmonic nanoparticles: The effect of the position of nanoparticles. Journal of Optoelectronical Nanostructures. 5(4), 17-32.

[3] Yin Z, Jing X, Li S (2024) Cascade amplification-based triple probe biosensor for highprecision DNA hybridization detection of lung cancer gene. APL Photonics 9:096111. https://doi.org/10.1063/5.0228760

[4] Karki B, Alsubaie AS, Sarkar P, Sharma M, Ali NB (2024) Detection of Skin, Cervical, and Breast Cancer Using Au–Ag Alloy and WS2−Based Surface Plasmon Resonance Sensor. Plasmonics. https://doi.org/10.1007/s11468-024-02521-z

[5] Rahimi H (2018) Absorption Spectra of a Graphene Embedded One Dimensional Fibonacci Aperiodic Structure. Journal of Optoelectronical Nanostructures. 4(3). 45-58

[6] Hossain B, Paul AK, Islam A, Rahman M, Sarkar AK, Abdulrazak LF (2022) A highly sensitive surface plasmon resonance biosensor using SnSe allotrope and heterostructure of BlueP/MoS2 for cancerous cell detection. Optik 252:168506. https://doi.org/10.1016/j.ijleo.2021.168506

[7] Rahman MS, Anower MS, Hasan MR et al (2017) Design and numerical analysis of highly sensitive Au-MoS2-graphene based hybrid surface plasmon resonance biosensor. Opt. Commun 396:36–43. https://doi.org/10.1016/j.optcom.2017.03.035

[8] Dey B, Islam S, Park J (2021) Numerical design of high-performance WS2/metal/WS2/graphene heterostructure based surface plasmon resonance refractive index sensor. Results Phys 23:104021. https://doi.org/10.1016/j.rinp.2021.104021

[9] Balbinot S, Srivastav AM, Vidic J, Abdulhalim I, Manzano M (2021) Plasmonic biosensors for food control. Trends Food Sci. Technol 111:128–140. https://doi.org/10.1016/j.tifs.2021.02.057

[10] Yan J, Wang L, Tang L, Lin L, Liu Y, Li J (2015) Enzyme-guided plasmonic biosensor based on dual-functional nano- hybrid for sensitive detection of thrombin. Biosens. Bioelectron 70:404-410 http://dx.doi.org/10.1016/j.bios.2015.03.024

[11] Hossain B, Paul AK, Islam A, Hossain F, Rahman M (2022) Design and analysis of highly sensitive prism based surface plasmon resonance optical salinity sensor. Results Opt 7:100217. https://doi.org/10.1016/j.rio.2022.100217

[12] Kretschmann E, Raether H (1968) Radiative decay of non-radiative surface plasmons excited by light. Z. Nat. A 23:2135–2136. https://doi.org/10.1515/zna-1968-1247

[13] Otto A (1968) Excitation of nonradiative surface plasma waves in silver by the method of frustrated total reflection. Z. Phys 216:398–410. https://doi.org/10.1007/BF01391532

[14] Yin Z, Jing X (2024) Visible-NIR surface plasmon resonance sensing technology for high precision refractive index detection. Opt. Lett 49:1477-1480. https://doi.org/10.1364/OL.520025

[15] Sayyad Tondro A, Sadeghi M, Kamaly A, Adelpour Z, Emamghorashi SA (2023) Design and Modeling of a D–Shaped PCF Refractive Index Sensor Based on SPR Effect. Journal of Optoelectronical Nanostructures. 8(3), 67-78. https://doi.org/10.30495/JOPN.2023.31381.1278

[16] Heidary Orojloo M, Jabbari M, Solookinejad G, Sohrabi F (2022) Design and modeling of photonic crystal Absorber by using Gold and graphene films. Journal of Optoelectronical Nanostructures. 7(2), 1-10. https://doi.org/10.30495/JOPN.2022.28915.1235

[17] Karki B, Trabelsi Y, Sarkar P, Pal A, Uniyal A (2025) Tuning sensitivity of surface plasmon resonance gas sensor based on multilayer black phosphorous. Mod. Phys. Lett. B 39:2450364. https://doi.org/10.1142/S0217984924503640

[18] Nur JN, Hasib MHH, Asrafy F, Shushama KN, Unum R, Rana MM (2019) Improvement of the performance parameters of the surface plasmon resonance biosensor using Al2O3 and WS2. Opt. Quant. Electron 51:1–11. https://doi.org/10.1007/s11082-019-1886-9

[19] Liu N, Wang S, Cheng Q, Pang B, Lv J (2021) High sensitivity in Ni-Based SPR sensor of blue phosphorene/transition metal dichalcogenides hybrid nanostructure. Plasmonics 16:1567–1576. https://doi.org/10.1007/s11468-021-01421-w

[20] Vibisha GA, Nayak JK, Maheswari P, Priyadharsini N, Nisha A, Jaroszewicz Z, Rajesh KB, Jha R (2020) Sensitivity enhancement of surface plasmon resonance sensor using hybrid configuration of 2D materials over bimetallic layer of Cu–Ni. Opt. Commun. 463:125337. https://doi.org/10.1016/j.optcom.2020.125337

[21] Karki B, Pal A, Singh Y, Sharma S (2022) Sensitivity enhancement of surface plasmon resonance sensor using 2D material barium titanate and black phosphorus over the bimetallic layer of Au, Ag, and Cu. Opt. Commun 508:127616. https://doi.org/10.1016/j.optcom.2021.127616

[22] Kumar R, Pal S, Verma A, Prajapati YK, Saini JP (2020) Effect of silicon on sensitivity of SPR biosensor using hybrid nanostructure of black phosphorus and MXene. Superlatt. Microstruct 145:106591. https://doi.org/10.1016/j.spmi.2020.106591

[23] Kumar A, Kumar A, Kushwaha AS, Dubey SK, Srivastava SK (2022) A comparative study of different types of sandwiched structures of SPR biosensor for sensitive detection of ssDNA. Photonics Nanostruct. Fundam. Appl 48:100984. https://doi.org/10.1016/j.photonics.2021.100984

[24] Wu L, Guo J, Wang Q, Lu S, Dai X, Xiang Y ,Fan D (2017) Sensitivity enhancement by using few-layer blackphosphorus-graphene/TMDCs heterostructure in surface plasmonresonance biochemical sensor. Sens. Actuators B 249:542–548. https://doi.org/10.1016/j.snb.2017.04.110

[25] Qiu M, Wang D, Liang W, Cao Y (2018) Novel concept of the smart NIR-light–controlled drug release of black phosphorus nanostructure for cancer therapy. Proc. Natl Acad. Sci 115:501–506. https://doi.org/10.1073/pnas.1714421115

[26] Manzeli S, Ovchinnikov D, Pasquier D, Yazyev OV, Kis A (2017) 2D transition metal dichalcogenides. Nat. Rev. Mater 2:17033. https://doi.org/10.1038/natrevmats.2017.33

[27] Kalpana N, Alodhayb AN, Pandiaraj S, Singh S (2025) Sensitivity Enhancement Using Surface Plasmon Resonance Sensor for Colorectal Detection by Employing Heterostructure. Plasmonics. https://doi.org/10.1007/s11468-024-02735-1

[28] Zahmatkeshan H, Karimi MJ, Sadeghi M, Adelpour Z (2025) Investigation and Optimization of the Sensitivity in a Franckeite-Based Biosensor with Bimetallic Layers. Plasmonics. https://doi.org/10.1007/s11468-025-02822-x

[29] Singh S, Sharma AK, Lohia P, Dwivedi DK (2021) Theoretical analysis of sensitivity enhancement of surface plasmon resonance biosensor with zinc oxide and blue phosphorus/ MoS2 heterostructure. Optik 244:167618. https://doi.org/10.1016/j.ijleo.2021.167618

[30] Panda, Pukhrambam PD (2022) Modeling of High-Performance SPR Refractive Index Sensor Employing Novel 2D Materials for Detection of Malaria Pathogens. IEEE Trans Nanobioscience. 21. https://doi.org/10.1109/TNB.2021.3115906

[31] Kumar A, Kumar A, Srivastava SK (2022) A study on surface plasmon resonance biosensor for the detection of CEA biomarker using 2D materials graphene, Mxene and MoS2. Optik 258:168885 https://doi.org/10.1016/j.ijleo.2022.168885

[32] Daher MG, Ahmed NM, Patel SK et al. (2023) Novel surface plasmon resonance detector for the detection of various alcohols with ultra-high sensitivity. Opt Quant Electron 55:1102. https://doi.org/10.1007/s11082-023-05418-z

[33] Li C, Li Z,, Guo S, Li X, Cheng Q, Meng S (2021) Sensitivity enhancement by employing BiFeO3 and graphene hybrid structure in surface plasmon resonance biosensors. Opt. Mater 121:111618. https://doi.org/10.1016/j.optmat.2021.111618

[34] Basak C, Hosain MK, Sazzad AA (2020) Design and simulation of a high sensitive surface plasmon resonance biosensor for detection of biomolecules. Sens. Imaging 21:1–19. https://doi.org/10.1007/s11220-019-0267-6

[35] Feng Y, Liu Y, Teng J (2018) Design of an ultrasensitive SPR biosensor based on a graphene-MoS 2 hybrid structure with a MgF2 prism. Appl. Opt 57:3639. https://doi.org/10.1364/AO.57.003639

[36] Kumar S, Yadav A, Malomed BA (2023) High performance surface plasmon resonance based sensor using black phosphorus and magnesium oxide adhesion layer. Front. Mater 10. https://doi.org/10.3389/fmats.2023.1131412

[37] Rikta KA, Anower MS, Rahman MS, Rahman MM (2021) SPR biosensor using SnSe-phosphorene heterostructure. Sens. Bio-Sens. Res 33:100442. https://doi.org/10.1016/j.sbsr.2021.100442

[38] Karki B, Sharma S, Singh Y, Pal A (2021) Sensitivity enhancement of surface plasmon resonance biosensor with 2-D franckeite nanosheets. Plasmonics 17:71-78. https://doi.org/10.1007/s11468-021-01495-6

[39] Dai X, Liang Y, Zhao Y, Gan S, Jia Y, Xiang Y (2019) Sensitivity enhancement of a surface plasmon resonance with tin selenide (SnSe) allotropes. Sensors 19:173. https://doi.org/10.3390/s19010173

[40] Singh S, Sharma AK, Lohia P, Dwivedi DK, Singh PK (2022) Design and modelling of high-performance surface plasmon resonance refractive index sensor using BaTiO3, MXene and nickel hybrid nanostructure. Plasmonics. 17(5), 2049-62. https://doi.org/10.1007/s11468-022-01692-x